

Unlocking the Capabilities of Vision-Language Models for Generalizable and Explainable Deepfake Detection

Peipeng Yu¹ Jianwei Fei² Hui Gao¹ Xuan Feng¹ Zhihua Xia¹ Chip-Hong Chang³

Abstract

This paper presents a novel deepfake detection framework based on Large Vision-Language Model (LVLM) that integrates external knowledge to improve generalization and explainability. Previous deepfake detection methods often rely on data or feature augmentation to increase diversity but lack the incorporation of human knowledge, which limits their ability to generalize across different forgery types and unseen manipulations. To address these limitations, we first train a generalized detector by introducing external knowledge, then fine-tune the LVLM to enable multi-turn dialogue capabilities. Our framework includes a Knowledge-guided Forgery Detector, an image encoder, and a Large Language Model (LLM). The image encoder extracts visual prompt embeddings from images, while the LLM receives visual and question prompt embeddings for inference. The Knowledge-guided Forgery Detection Module is used to calculate correlations between image features and pristine/deepfake class embeddings, enabling forgery classification and localization. The outputs from these components are processed by a Forgery Prompt Learner to construct forgery prompt embeddings. Finally, we feed these prompt embeddings into the LLM to generate textual detection response to assist judgment. Extensive experiments on multiple benchmarks, including FF++, CDF2, DFD, DFDCP, and DFDC, demonstrate that our scheme surpasses state-of-the-art methods in generalization performance, while also supporting multi-turn dialogue capabilities.

1. Introduction

The rapid advancement of generative artificial intelligence has significantly accelerated the development of deepfake technology, facilitating realistic facial manipulation and reenactment. While these technologies have notable applications in the entertainment and art fields, such as Stable Diffusion (Esser et al., 2024) and DALL-E (Ramesh et al.,

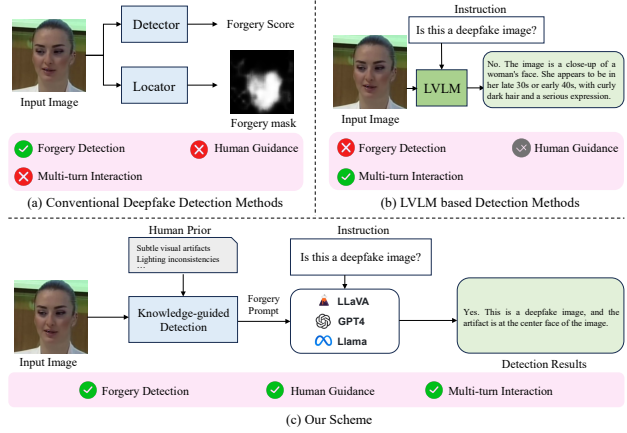


Figure 1. Comparison of existing deepfake detection methods. Existing approaches can perform localization and classification but ignore integrating external knowledge. Our scheme introduces a Knowledge-guided detection module to enhance generalization capabilities, and enables multi-turn dialogues.

2021), their misuse poses critical security risks to society (Wang et al., 2024b). These tools allow users to synthesize realistic but nonexistent content by merely inputting carefully designed prompts, making deepfake generation more accessible and potentially dangerous than ever before.

Current deepfake detection research primarily focuses on enhancing generalization and accuracy for identifying previously unseen forgeries. Various approaches have been explored, including feature consistency analysis (Dong et al., 2022; Zhao et al., 2021b; Liu et al., 2023), reconstruction error techniques (Cao et al., 2022; Chen et al., 2021; Shi et al., 2023), and methods focusing on visual artifacts (Wang et al., 2023b; Sun et al., 2023; Nguyen et al., 2024). While these methods effectively leverage image-level or feature-level anomalies, they often struggle to fulfill interpretability requirements in real-world scenarios. In judicial settings, however, existing deepfake detection systems must also support conversational capabilities to address inquiries from judges and skeptics. Consequently, the key challenge lies in providing sufficient interpretability without compromising generalization performance.

Thus, our objective is to develop a generalized and explain-

able deepfake detection scheme. Large Vision-Language Models (LVLMs) presents a promising leverage to this issue. Pre-trained on extensive and diverse datasets, LVLMs capture vast amounts of knowledge about natural objects, providing significant potential to improve generalization in identifying manipulated content. Furthermore, LVLMs exhibit capabilities for effective learning in low-sample scenarios, making them particularly suitable for tasks with limited annotated data (Xu et al., 2024; Huang et al., 2024). A LVLM typically uses an image encoder to extract image features, which are then combined with text prompts and input into the Large Language Model (LLM) to generate responses. For instance, inputting an image along with a prompt like *“This is a facial image designed for deepfake detection, and it should not exhibit any localized color discrepancies. Is this a deepfake image?”* allows the LVLM to assess potential manipulations. However, existing LVLMs are primarily optimized for general image understanding tasks and may not effectively capture the fine-grained features required for deepfake detection. Directly performing fine-tuning presents challenges, as the LVLM may struggle to interpret specialized terms like *“visual artifacts”* or *“inconsistencies”* as intended in the context of forgery detection. Therefore, it is crucial to design fine-grained prompt embeddings to facilitate LVLM training.

To address these challenges, we propose a novel LVLM-based deepfake detection framework under the guidance of pretrained knowledge of LVLM to make generalizable and explainable detection (Lester et al., 2021; Liu et al., 2022). As shown in Figure 1, we first integrate external knowledge to train a generalizable detector, and then incorporate its features into LLM to generate responses. Specifically, the framework comprises two key stages: Knowledge-guided Forgery Detector Training and LLM Prompt Tuning. In the Knowledge-Guided Forgery Detector Training phase, we aim to train a high-precision deepfake detector. Leveraging a pre-trained multimodal model, we extract both image content features and textual features from descriptions of real and fake images. By calculating the correlation between these image features and learnable real/fake class embeddings, we generate consistency maps that represent the alignment between visual content and textual descriptions. These maps are subsequently processed by the Forgery Locator and Classifier to produce a forgery segmentation map and forgery score. Subsequently, in the LLM Prompt Tuning phase, we incorporate deepfake detection knowledge into the LLM to generate forgery detection descriptions. To ensure accurate deepfake detection, we train the LVLM using simulated forgery image-text pairs specifically tailored for this task. Our contributions are summarized as follows:

- We propose a novel LVLM-based framework for deepfake detection that integrates fine-grained forgery prompt embeddings through prompt tuning, which sig-

nificantly enhances model generalization and explainability.

- We introduce a Knowledge-guided Forgery Detector to generate forgery consistency maps to align image features with textual descriptions of both pristine and deepfake images for enhanced generalization.
- Extensive experiments on multiple benchmarks, including FF++, CDF1, CDF2, DFD, DFDCP, and DFDC, demonstrate that our scheme outperforms existing methods in generalization performance, with the added capability of supporting multi-turn dialogue.

2. Related Works

Deepfake Detection Methods: Conventional classification architectures have achieved significant success in detecting forgery clues in early deepfake methods. Various strategies, such as data augmentation (Li et al., 2020a; Shiohara & Yamasaki, 2022; Nguyen et al., 2024), feature consistency analysis (Zhao et al., 2021b; Yan et al., 2023), and frequency domain anomaly detection (Jeong et al., 2022; Liu et al., 2021; Wang et al., 2023a), have been explored in recent years to enhance the generalization of deepfake detection models. While these methods achieve a high detection accuracy, they primarily rely on data augmentation or enhanced feature extraction (Yan et al., 2024), and often neglect the integration of external human knowledge. However, many deepfake characteristics are embedded in human knowledge, which is challenging to capture through data or feature augmentation alone. This limitation significantly constrains the generalization capabilities of existing algorithms. In this paper, we propose an LVLM-based deepfake detection framework that aligns image features with real/fake descriptions to enhance the model’s capacity to detect unseen deepfakes.

Large Vision-Language Models: Recent advancements in Large Vision-Language Models (LVLMs) have showcased their potential in multimodal tasks (Gunjal et al., 2024; Leng et al., 2024; Gu et al., 2024). A typical LVLM architecture comprises an image encoder, a projector, and a LLM. The image encoder extracts visual features from input images, which are then transformed by the projector into visual prompt embeddings. These visual embeddings, combined with textual prompt embeddings, are fed into the LLM to generate responses. Building on this architecture, models such as BLIP-2 (Li et al., 2023), LLaVA (Liu et al., 2024a), and MiniGPT-4 (Zhu et al., 2024) have achieved notable advancements in language instruction following (Su et al., 2023; Yang et al., 2024) and visual reasoning (Chen et al., 2024) for natural scenes. Some studies have also explored the application of LVLMs in forgery detection. FakeShield (Xu et al., 2024) constructed a large-scale

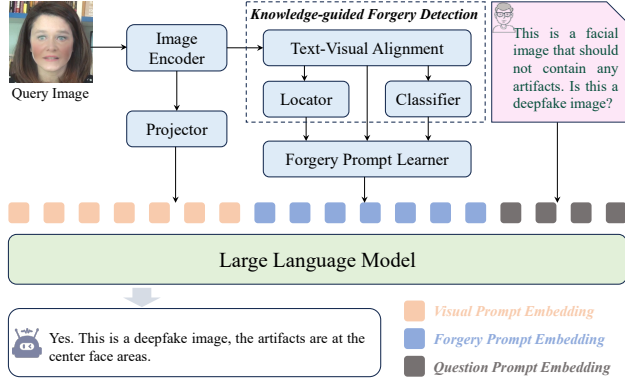


Figure 2. Overview of the proposed framework. The framework consists of three main components: (1) a Knowledge-guided Forgery Detection module, structured as a multi-task learning framework comprising three parts: a Visual-text alignment module, a forgery classifier, and a forgery locator. (2) a Forgery Prompt Learner, which is designed to fuse forgery detection outputs and generate forgery prompt embeddings. (3) a Large Language Model (LLM), which utilizes the extracted question, visual, and forgery prompt embeddings to generate responses.

image-text dataset and introduced an LVLM-based framework specifically designed for forgery detection. FKA-Owl (Liu et al., 2024b) proposed a novel fake news detection framework that leverages forgery-specific knowledge to augment LVLMs, enabling them to reason about manipulations. Similarly, FFAA (Huang et al., 2024) proposed a multi-modal LVLM approach for explainable, open-world face forgery analysis, highlighting the potential of LVLMs in forgery detection tasks.

Despite these advancements, current LVLMs primarily focus on general language processing and visual understanding, often missing the fine-grained details that are essential for deepfake detection tasks. This limitation restricts their effectiveness in forgery localization and classification. To bridge this gap, we develop a novel deepfake detection framework based on LVLMs that constructs fine-grained forgery prompt embeddings to guide the LLM in detecting subtle manipulations. By integrating rich external knowledge in the pretrained LVLM, our scheme could enhance generalization across diverse forgery types while retaining the model’s original dialogue capabilities.

3. Proposed Method

Our objective is to enable LVLMs to accurately distinguish between real and fake faces. Although LVLMs are trained on large-scale datasets, they are primarily trained for general image understanding tasks and often lack the sensitivity for detecting forgery details. To address this limitation, we propose a novel LVLM-based deepfake detection frame-

work that enhances sensitivity to deepfake artifacts through constructing fine-grained forgery prompts. As shown in Figure 2, our scheme builds upon a conventional LVLM framework, which comprises an image encoder, a projector, and an LLM. The image encoder extracts content features from input images, which are subsequently transformed into visual prompt embeddings E_{visual} by the projector. Additionally, user queries are tokenized into question prompt embeddings $E_{question}$. To train the model for forgery detection, we employ a two-stage process. In the first stage, we train a Knowledge-guided Forgery Detector (KFD) to perform forgery detection and localization by calculating the correlation between image content features and deepfake descriptions. This stage ensures that the KFD can effectively classify and localize forgery artifacts by learning fine-grained visual-text correlations. In the second stage, we perform LLM Prompt Tuning to integrate the KFD knowledge into the LVLM framework. Specifically, we design a Forgery Prompt Learner to convert forgery-related features into forgery prompt embeddings. These embeddings, along with the question and visual prompt embeddings, are then fed into the LLM to generate a textual detection result. By employing prompt tuning and alternating training with pre-trained data, our scheme ensures accurate deepfake detection while preserving the LLM’s multi-turn dialogue capability.

3.1. Knowledge-guided Forgery Detector

Forgery Visual-Text Alignment: To acquire forgery detection-related knowledge, inspired by (Jeong et al., 2023), we align image content features with predefined text description features to obtain fine-grained forgery features. This process is illustrated in Figure 3. Specifically, this process involves a pretrained image encoder, a pretrained text encoder, and a linear layer. Both the image and text encoders are sourced from ImageBind, a large-scale multimodal pre-trained model with extensive cross-modal knowledge. We first define real and fake image descriptions, D_{real} and D_{fake} , and augment them with learnable context to enable the Text Encoder to extract task-relevant textual features, $F_{text} \in \mathbb{R}^{2 \times C_{text}}$. For the visual features, we select l layers from the image encoder and obtain the intermediate features extracted by each selected layer. The extracted features are then processed by a linear layer to generate visual features $F_{vis}^i \in \mathbb{R}^{H_i \times W_i \times C_{text}}$, where i indicates the i -th layer. The similarity maps between visual features and textual features are calculated and concatenated as consistency maps. The formula for computing the consistency maps is as follows:

$$C_{text} = \{F_{vis}^i F_{text}^T\}. \quad (1)$$

Additionally, to optimize the extracted image features, we compute the similarity between the features of a reference image (pristine image) F_{vref}^i and the input image features

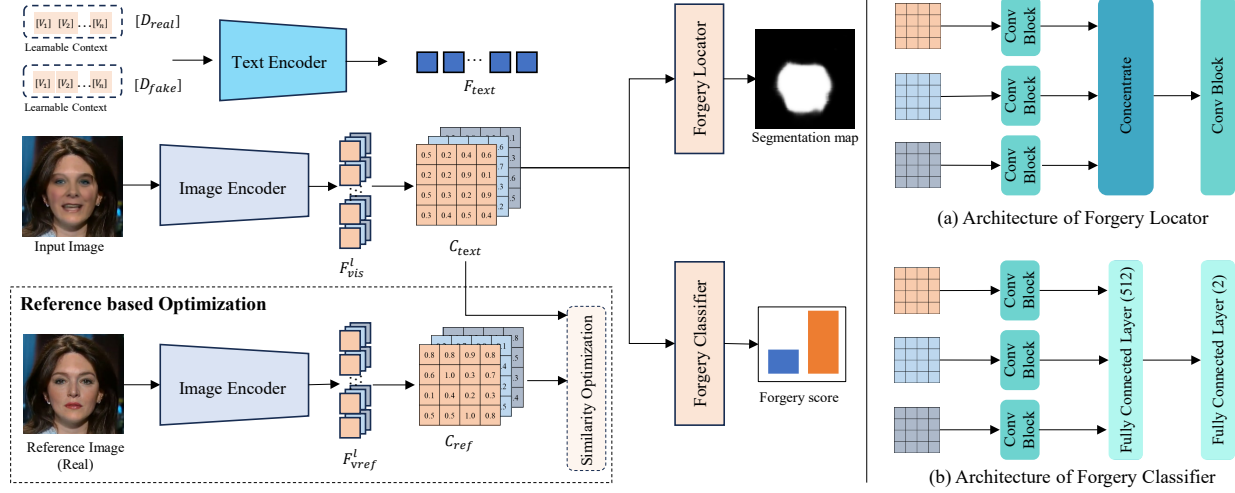


Figure 3. Overview of the Knowledge-guided Forgery Detector. It uses a pretrained image encoder and text encoder to extract features from both modalities, and computes their correlation to produce consistency maps. These maps are further processed by a forgery classifier and a locator, yielding a forgery score and a forgery segmentation map. The Reference based Optimization process is applied exclusively during the training phase to enhance the robustness of extracted features.

F_{vis}^i . This similarity optimization enhances the robustness of the features extracted by the image encoder. Note that reference images are used only during training and are not employed at test time. The similarity is calculated as:

$$C_{ref} = \{Cos(F_{vref}^i, F_{vis}^i)\}. \quad (2)$$

Forgery Locator and Classifier: To enhance the model’s sensitivity to deepfake content, we introduce a Forgery Locator and a Forgery Classifier to locate forgery areas and classify pristine and deepfake images. As shown in Figure 3, the Forgery Locator consists of three branches. Each branch applies down-sampling and up-sampling operations on the corresponding consistency maps, followed by concatenation and convolution operations to generate the segmentation map. The Forgery Classifier also consists of three branches. The three feature maps after convolution are down-sampled before they are concatenated. After that, we use two fully connected layers to calculate the probability of the image being real or fake. Here, we use Dice Loss to improve the accuracy of forgery segmentation. We further enhance the robustness of extracted forgery features by calculating the matching degree between segmentation maps for the textual consistency map (C_{text}) and the reference map (C_{ref}). Both maps are expected to accurately localize the forged regions. The localization loss is formulated as follows:

$$\mathcal{L}_{loc} = Dice(\phi(C_{text}), gt) + \lambda Dice(\phi(C_{ref}), gt), \quad (3)$$

where ϕ is the Forgery Locator, and gt is the ground truth mask. Dice loss measures the overlap between the predicted segmentation and the ground truth. λ is the loss weight for balancing these two losses.

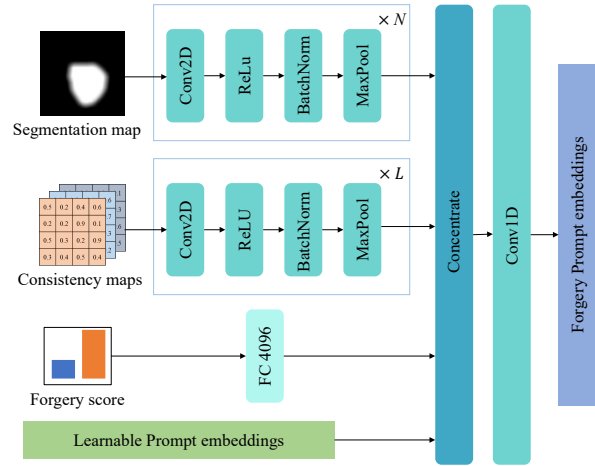


Figure 4. Architecture of the Forgery Prompt Learner.

Additionally, we use binary cross-entropy loss to optimize the performance of the forgery classification task. The formula is as follows:

$$\mathcal{L}_{cls} = -(c \log(\hat{c}) + (1 - c) \log(1 - \hat{c})), \quad (4)$$

where \hat{c} is the predicted forgery score that the image is fake, and c is the ground truth label (0 for real and 1 for fake).

3.2. Forgery Prompt Learner and LLM

Forgery Prompt Learner: To effectively convert forgery-related features into inputs for the LLM, we propose a Forgery Prompt Learner to transform the forgery localization map, the forgery score, and the consistency maps

into forgery prompt embeddings. At the same time, we add a learnable prompt embeddings for the forgery prompt learner to incorporate extra information for the deepfake detection task. As shown in Figure 4, the Forgery Prompt Learner consists of two convolutional neural networks, one fully connected layer, and the learnable prompt embeddings $E_{base} \in \mathbb{R}^{n_1 \times C_{emb}}$. Specifically, the two convolutional networks transform the forgery localization map and consistency maps into vector representations, $E_{loc} \in \mathbb{R}^{n_2 \times C_{emb}}$ and $E_{cons} \in \mathbb{R}^{n_3 \times C_{emb}}$, respectively. The forgery score is expanded into $E_{cls} \in \mathbb{R}^{1 \times C_{emb}}$. These embeddings are concatenated and fed into the convolution layer to generate the forgery prompt embeddings $E_{forgery} \in \mathbb{R}^{n_f \times C_{emb}}$. Finally, the forgery prompt embeddings, visual prompt embeddings, and question prompt embeddings are input into the LLM.

LLM: The LLM processes the prompt embeddings to interpret the context and accurately identify forged regions. By integrating visual details (from $E_{forgery}$ and E_{visual}) with user queries (from $E_{question}$), the LLM produces responses that provide forgery detection judgments and precisely localize manipulated regions (e.g., eyes, mouth). To optimize model performance, we employ prompt tuning on the LLM using simulated image-text pairs specifically designed for deepfake detection. To ensure the LLM generates accurate responses, we use cross-entropy loss to quantify the discrepancy between the predicted response and the target label. The formula is defined as follows:

$$\mathcal{L}_{llm} = - \sum_j y_j \log(\hat{y}_j), \quad (5)$$

where \hat{y}_j and y_j are the predicted probability, and the corresponding ground truth label, respectively for the j -th token in the sequence.

3.3. Data for LLM Prompt Tuning

Forgery Data Simulation: We intend for the LLM to identify pristine and deepfake images, while also locating the forged regions. This requires training on image-text pairs specifically depicting manipulated areas, which are currently unavailable. To address this gap, we draw on techniques from SBI (Shiohara & Yamasaki, 2022) to construct image-text pairs using existing real images. First, we generate facial landmarks from a real image I_{real} , then randomly select 1 to 3 regions (e.g., the nose, mouth, or eyes) as target forgery areas. We apply a slight affine transformation to the real image, resulting in an affine-transformed image I_{affine} . The original real image is used as the background (target face), and the affine-transformed image serves as the foreground (source face). Following the approach in (Nguyen et al., 2024), we apply Poisson blending to combine the foreground and background images. The blending process is defined as follows:

$$I_M = M \odot I_{affine} + (1 - M) \odot I_{real}, \quad (6)$$

where M is the Convex Hull mask constructed based on the selected forgery region, with values ranging from 0 to 1. The symbol \odot denotes element-wise multiplication.

Question and Answer Content: Training an LVLM requires a large number of visual question-answer pairs. Therefore, we construct corresponding text queries for each image. To ensure compatibility with the deepfake detection task, we first include a background description in each query, for example: “*This is a facial image designed for deepfake detection, and it should not exhibit any localized color discrepancies or evident signs of splicing.*”, which can be regarded as a kind of human prior knowledge. Additionally, we incorporate the prediction results from the Knowledge-Guided Forgery Detector (KFD) into the prompt, such as *According to KFD prediction, the forgery score is 0.93*. We then ask a question related to the content of the image, such as “*Is this a deepfake image?*” The LVLM’s response states whether a forgery is present in the image and where the forgery area is. For instance, “*Yes. This is a deepfake image, and the artifact is at the center face of the image.*” Here, the forgery regions are defined according to those selected during forgery data simulation. By defining both queries and responses, we can train the LVLM to distinguish between pristine and deepfake images. The prompt format input to the LVLM follows this format:

```
###Human: <Img>E_visual</Img>E_forgery[Task
description][KFD result] Is this a
deepfake image? ###Assistant:
```

where E_{visual} represents visual prompt embeddings, $E_{forgery}$ denotes the forgery prompt embeddings learned by the Forgery Prompt Learner, *KFD result* indicates the forgery score, and *Task description* provides a textual description of deepfake detection task.

4. Experiments

4.1. Experimental Settings

Datasets. The FaceForensics++ (FF++) (Rossler et al., 2019) dataset includes 1,000 real videos and 5,000 forgery videos across five deepfake categories, which is one of the most widely-used datasets for deepfake detection. DFD (Dufour & Gully, 2019), CDF1, CDF2 (Li et al., 2020b), DFDCP (Dolhansky, 2019), and DFDC (Dolhansky et al., 2020) are commonly used datasets for evaluating generalization performance in deepfake detection. The images are all cropped using Dlib and RetinaFace. To be consistent with the previous deepfake detection approaches, we trained only on real data from the FF++ dataset.

Evaluation Metrics. Following existing approaches (Shiohara & Yamasaki, 2022; Nguyen et al., 2024), we used the video-level Area Under the Receiver Operating Char-

Methods		Intra-dataset		Cross-dataset									
		FF++		CDF2		DFD		DFDC		CDF1		DFDCP	
		AUC	AP	AUC	AP	AUC	AP	AUC	AP	AUC	AP	AUC	AP
Xception (Rossler et al., 2019)	CVPR'19	97.23	96.44	81.65	88.74	89.75	-	-	-	80.98	90.00	69.90	81.95
FaceXRay+BI (Li et al., 2020a)	CVPR'20	-	-	79.50	-	95.40	93.34	-	-	80.58	73.33	80.92	72.65
F3Net (Qian et al., 2020)	ECCV'20	98.20	96.17	78.88	86.23	93.33	97.70	71.77	71.99	81.11	89.61	73.50	79.30
Multiattentional (Zhao et al., 2021a)	CVPR'21	-	-	68.26	-	92.95	-	-	-	-	-	63.02	-
SPSL (Liu et al., 2021)	CVPR'21	96.91	89.37	79.86	87.83	96.12	98.20	66.16	71.13	85.02	92.17	75.86	82.64
PCL+I2G (Zhao et al., 2021b)	CVPR'21	99.11	-	90.03	-	99.07	-	-	-	-	-	74.27	-
RECCE (Cao et al., 2022)	CVPR'22	99.32	97.25	82.31	88.26	98.26	98.40	69.58	69.98	81.49	89.04	71.49	77.04
SBI (Shiohara & Yamasaki, 2022)	CVPR'22	99.15	99.15	93.82	92.99	96.32	96.13	74.47	74.09	<u>93.44</u>	<u>93.77</u>	<u>90.95</u>	85.98
SFDG (Wang et al., 2023a)	CVPR'23	-	-	75.83	-	88.00	-	-	-	-	-	73.63	-
AltFreezing (Wang et al., 2023b)	CVPR'23	93.81	<u>98.74</u>	89.50	87.41	98.50	94.59	64.75	67.52	88.48	92.79	64.05	76.22
CADDM (Dong et al., 2023)	CVPR'23	99.70	-	93.88	-	99.03	-	73.85	-	85.68	-	74.19	-
UCF (Yan et al., 2023)	CVPR'23	98.69	97.99	83.73	90.10	94.50	98.04	75.11	<u>74.76</u>	86.08	91.78	80.50	77.16
TALL (Xu et al., 2023)	ICCV'23	<u>99.87</u>	-	90.79	-	-	-	76.78	-	-	-	-	-
LSDA (Yan et al., 2024)	CVPR'24	-	-	91.10	-	-	-	<u>77.00</u>	-	-	-	-	-
LAANet (Nguyen et al., 2024)	CVPR'24	99.96	-	95.40	97.64	<u>99.51</u>	<u>99.40</u>	-	-	-	-	86.94	97.70
Ours		99.53	99.54	<u>94.71</u>	<u>93.59</u>	99.64	99.68	79.12	77.69	97.62	97.67	91.81	<u>88.26</u>

Table 1. Intra-dataset and cross-dataset evaluation of KFD compared with existing deepfake detection methods. The highest AUC and AP scores among all methods are highlighted in **bold**, while the second-highest scores are underlined. All experimental results are sourced from the original papers or publicly available code repositories.

acteristic Curve (AUC) and Average Precision (AP) as our evaluation metric. Additionally, we assess the LLM’s performance by evaluating the binary classification (Yes or No) of authenticity in its textual output, allowing us to calculate a corresponding video-level AUC for the LLM’s responses.

Compared Methods. We evaluated our approach against several state-of-the-art deepfake detection algorithms (Rossler et al., 2019; Li et al., 2020a; Zhao et al., 2021a; Liu et al., 2021; Zhao et al., 2021b; Cao et al., 2022; Shiohara & Yamasaki, 2022; Wang et al., 2023a;b; Dong et al., 2023; Yan et al., 2023; Qian et al., 2020; Nguyen et al., 2024) and LVLM-Based Methods (Khan & Dang-Nguyen, 2024; Su et al., 2023; Liu et al., 2024b; Wang et al., 2024a).

Implementation Details. Our approach leverages the PandaGPT architecture, which incorporates the ImageBind-Huge model as the image and text encoder. We extract features from the 16th, 24th, and 32nd layers of the encoder to compute consistency maps with the text features, which are then passed to the Vicuna-7B model for inference. For multi-turn dialogue capability, we alternate training between the deepfake dataset and the PandaGPT dataset. All the images are cropped to 224×224 . Training is conducted on two Nvidia RTX 4090 GPUs over 50 epochs, using the Adam optimizer with a learning rate of $1e-4$ and a weight decay of $1e-5$.

4.2. Comparison with SOTA Detection Methods

We first compare our approach with several state-of-the-art deepfake detection methods (Li et al., 2020a; Shiohara &

Yamasaki, 2022; Cao et al., 2022; Huang et al., 2023; Yan et al., 2024; Tan et al., 2024).

Intra-Dataset Evaluation. Following the intra-dataset protocol outlined in (Yan et al., 2024; Nguyen et al., 2024), we compare our approach with existing state-of-the-art deepfake detection methods based on the outputs of KFD. As shown in Table 1, our method achieves competitive results, reaching a detection AUC of 99.53% on the FF++ dataset.

Cross-Dataset Evaluation. Following previous works (Li et al., 2020a; Shiohara & Yamasaki, 2022; Nguyen et al., 2024), we further perform a cross-dataset evaluation. The models are trained on real data from the FF++ dataset, and the detection performance is assessed on CDF1, CDF2, DFD, DFDCP, and DFDC datasets. We report video-level AUC and AP scores across these datasets. The results are summarized in Table 1. Our model surpasses the best existing methods, achieving a performance gain in detection AUC of 2.12%, and 4.18% on the DFDC, and CDF1 datasets, respectively. Overall, our approach provides a mean improvement of 1.34% in AUC, highlighting its generalization ability across diverse datasets.

GradCAM Visualization. In this section, we use GradCAM (Selvaraju et al., 2017) to visualize attention during deepfake detection. As shown in Figure 5, we compare our method with SBI (Shiohara & Yamasaki, 2022) across the CDF2, DFD, and DFDC datasets. While SBI can detect forged regions, it may misidentify these areas and tends to highlight irrelevant regions when encountering unknown forgeries. In contrast, our scheme, guided by external knowl-

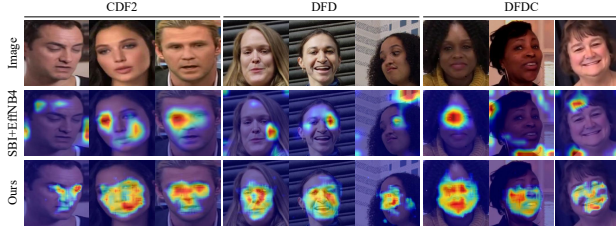


Figure 5. GradCAM visualizations on the CDF2, DFD, and DFDC datasets.

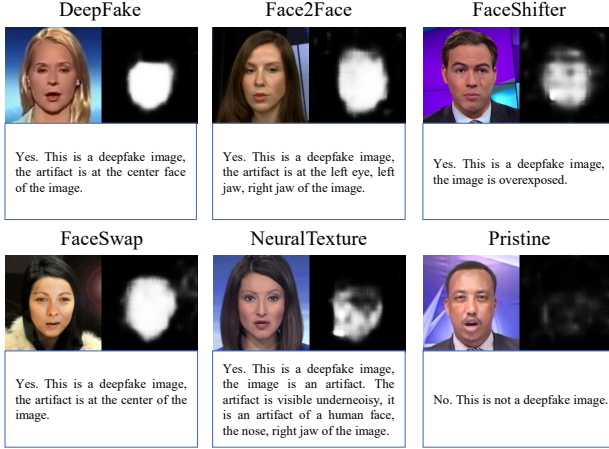


Figure 6. Forgery localization results and LLM responses on various forgery types from the FF++ dataset. For each example, the top-left shows the original image, the top-right displays the forgery segmentation map, and the text below provides the LLM’s textual detection result.

edge, effectively identifies regions that are inconsistent with predefined textual descriptions.

4.3. Comparison with LVLM-based Methods

Detection Performance of LVLM. We further benchmark our framework against leading LVLM-based methods (Zhou et al., 2022; Su et al., 2023; Wang et al., 2024a). In these evaluations, both the image and the query are provided as inputs to the LVLM, with the model tasked to determine the authenticity of the image (real or fake). For PandaGPT, Qwen2-VL, and our scheme, we utilize the LLM’s output (“Yes” or “No”) to classify authenticity, and subsequently compute the AUC values for evaluation. As shown in Table 2, compared to existing LVLM-based approaches, our model shows superior results, achieving a performance improvement of 5% , 9%, 3%, 14% ,and 10% on the FF++, CDF2, DFD, CDF1, and DFDCP datasets, respectively.

Dialogues Visualization. Unlike prior detection methods, our approach not only supports deepfake detection but also facilitates multi-turn dialogues, enabling users to further

Methods	FF++	CDF2	DFD	CDF1	DFDCP	Avg
P-Tuning	<u>91.32</u>	<u>79.97</u>	<u>88.74</u>	<u>81.45</u>	<u>69.26</u>	<u>82.15</u>
PandaGPT	63.42	62.53	64.56	55.01	46.06	58.32
Qwen2-VL	50.50	48.88	42.38	46.46	51.71	47.99
FAK-Owl	67.54	73.51	68.61	62.13	65.96	67.55
Ours-LLM	97.11	89.90	92.26	95.97	86.70	92.39
Ours-VLM	97.11	89.90	92.26	95.97	86.70	92.39

Table 2. **Comparison of our scheme with existing LVLM-based methods.** All AUC values are calculated based on textual outputs generated by the LVLM. P-Tuning (Khan & Dang-Nguyen, 2024) and PandaGPT (Su et al., 2023) are fine-tuned on the FF++ dataset, FAK-Owl (Liu et al., 2024b) is trained based on original image-text pairs, and Qwen2-VL (Wang et al., 2024a) is evaluated with its original pre-trained weights. The best and second-best results are highlighted in **bold** and underlined, respectively.

Training Number	Test set AUC				
	FF++	CDF1	DFD	DFDC	Avg
50	92.68	83.18	74.46	61.82	78.04
100	94.38	91.12	78.99	63.88	82.09
200	94.02	91.98	80.47	62.09	82.14
500	95.15	91.82	81.65	65.31	83.48

Table 3. **Generalization evaluation across different numbers of training images.**

inquire about the image content. Figure 6 presents some example dialogues on the FF++ dataset. It shows that our proposed scheme accurately identifies forged regions within the images, while the LLM provides precise and contextually relevant judgments. Additional multi-turn dialogue examples are provided in the supplementary material.

4.4. Analysis

Number of Training Images. Obtaining large-scale face images in real-world scenarios is often infeasible. Hence, we assess our model’s performance with varying numbers of training images. Specifically, we randomly sample 50, 100, 200, and 500 real images from FF++ to create corresponding fake image-text pairs for training. As shown in Table 3, our approach achieves state-of-the-art performance using only 500 training images. Although reducing the training set size leads to a slight degradation in accuracy, our method still maintains competitive results with as few as 100 training images. This underscores the robustness of our framework, particularly in scenarios where data are scarce.

Effect of Prompt Tuning. The prompt tuning process is designed to convert forgery detection knowledge into the input of LLM to facilitate accurate detection. This process involves the Forgery Prompt Learner (FPL), the LLM, and the LoRA strategy. To evaluate the effectiveness of this com-

FPL	LLM	Lora	FF++		CDF2		DFDC	
			AUC	AP	AUC	AP	AUC	AP
	✓		50.00	50.00	50.28	65.56	50.00	49.93
	✓	✓	63.42	61.22	62.53	59.02	55.11	53.47
✓	✓		96.59	96.13	89.25	94.69	67.65	64.07
✓	✓	✓	97.11	96.97	89.90	94.51	68.77	64.57

Table 4. **Ablation study results on FF++, CDF2, and DFDC.** The ✓ in the FPL column indicates the inclusion of forgery prompt embeddings in the framework. The ✓ in the LLM column signifies the use of an LLM for inference, while the ✓ in the LoRA column denotes whether LoRA is used to fine-tune the LLM.

Training Set		Test Set AUC (%)					
Database	#Real	FF++	CDF2	DFDCP	DFDC	Avg	
FF++	720	99.54	94.32	92.39	77.03	90.82	
CDF2	622	97.95	95.79	86.36	70.27	87.59	
DFDCP	737	99.15	85.17	93.74	69.64	86.93	

Table 5. **Generalization evaluation across various training datasets.**

ponent, we conducted ablation experiments on four subsets of FF++ as well as CDF2 and DFDCP datasets. For each configuration, the AUC was calculated based on the LLM’s output in determining real versus fake images. As shown in Table 4, models equipped with the Forgery Prompt Learner demonstrate higher AUC values, indicating improved effectiveness for deepfake detection tasks. Furthermore, the integration of LoRA further enhances performance, achieving superior results across multiple datasets compared to configurations without LoRA.

Generalizability to Training Datasets. The generalizability of deepfake detection is closely tied to the diversity of the training data used. To verify the effectiveness of our approach across different datasets, we trained the model on various training sets and conducted cross-dataset evaluation on FF++, CDF2, DFDCP, and DFDC datasets. We calculated detection AUC and AP values based on the LLM’s responses, as shown in Table 5. The results indicate that our method exhibits strong robustness across diverse datasets and demonstrates its ability to generalize across different types of forgeries using varied real data.

Effects of different LLM architectures. The deepfake detection performance is closely related to the specific LLM architecture used, as different LLMs exhibit unique characteristics. To examine detection performance across various LLM architectures, we evaluated three models: Llama-3.2-1B, Llama-3.2-3B, and Vicuna-7B. The evaluation is conducted on the FF++, CDF1, DFD, and DFDC datasets. As shown in Table 6, larger-scale architectures consistently achieved better detection performance, indicating that models with greater parameter counts are better suited to capturing

LLM Architecture	Test set AUC				
	FF++	CDF1	DFD	DFDC	Avg
Llama-3.2-1B	96.49	95.64	82.74	65.66	85.13
Llama-3.2-3B	97.08	95.30	82.80	66.12	85.32
Vicuna-7B	97.11	95.97	84.26	67.65	86.25

Table 6. **Generalization evaluation across different LLM architectures.** The AUC is computed based on the LLM output.

ing subtle forgery artifacts.

5. Conclusion

In this work, we introduced a novel deepfake detection framework that leverages Large Vision-Language Models (LVLMs) to enhance generalization and explainability. By integrating a Forgery Vision-Text Alignment Module, we effectively align image features with textual descriptions of pristine and deepfake images to facilitate the generation of forgery consistency maps. Additionally, we incorporated a Forgery Prompt Learner capable of transforming fine-grained forgery features into inputs for the LLM, enabling accurate forgery detection responses. Extensive evaluations across multiple benchmarks, including FF++, CDF1, CDF2, DFD, DFDCP, and DFDC, demonstrate that our scheme outperforms existing methods in generalization performance. These findings underscore the potential of LVLM-based approaches in advancing deepfake detection methodologies.

References

- Cao, J., Ma, C., Yao, T., Chen, S., Ding, S., and Yang, X. End-to-end reconstruction-classification learning for face forgery detection. In *Proceedings of the IEEE/CVF Conference on Computer Vision and Pattern Recognition*, pp. 4113–4122, 2022.
- Chen, L., Li, B., Shen, S., Yang, J., Li, C., Keutzer, K., Darrell, T., and Liu, Z. Large language models are visual reasoning coordinators. *Advances in Neural Information Processing Systems*, 36, 2024.
- Chen, Z., Xie, L., Pang, S., He, Y., and Zhang, B. Magdr: Mask-guided detection and reconstruction for defending deepfakes. In *Proceedings of the IEEE/CVF Conference on Computer Vision and Pattern Recognition*, pp. 9014–9023, 2021.
- Dolhansky, B. The dee pfake detection challenge (dfdc) pre view dataset. *arXiv preprint arXiv:1910.08854*, 2019.
- Dolhansky, B., Bitton, J., Pflaum, B., Lu, J., Howes, R., Wang, M., and Ferrer, C. C. The deepfake detection challenge (dfdc) dataset. *arXiv preprint arXiv:2006.07397*, 2020.

- Dong, S., Wang, J., Ji, R., Liang, J., Fan, H., and Ge, Z. Implicit identity leakage: The stumbling block to improving deepfake detection generalization. In *Proceedings of the IEEE/CVF Conference on Computer Vision and Pattern Recognition*, pp. 3994–4004, 2023.
- Dong, X., Bao, J., Chen, D., Zhang, T., Zhang, W., Yu, N., Chen, D., Wen, F., and Guo, B. Protecting celebrities from deepfake with identity consistency transformer. In *Proceedings of the IEEE/CVF Conference on Computer Vision and Pattern Recognition*, pp. 9468–9478, 2022.
- Dufour, N. and Gully, A. Deepfakes detection dataset., 2019.
- Esser, P., Kulal, S., Blattmann, A., Entezari, R., Müller, J., Saini, H., Levi, Y., Lorenz, D., Sauer, A., Boesel, F., et al. Scaling rectified flow transformers for high-resolution image synthesis. In *Forty-first International Conference on Machine Learning*, 2024.
- Gu, Z., Zhu, B., Zhu, G., Chen, Y., Tang, M., and Wang, J. Anomalygpt: Detecting industrial anomalies using large vision-language models. In *Proceedings of the AAAI Conference on Artificial Intelligence*, volume 38, pp. 1932–1940, 2024.
- Gunjal, A., Yin, J., and Bas, E. Detecting and preventing hallucinations in large vision language models. In *Proceedings of the AAAI Conference on Artificial Intelligence*, volume 38, pp. 18135–18143, 2024.
- Huang, B., Wang, Z., Yang, J., Ai, J., Zou, Q., Wang, Q., and Ye, D. Implicit identity driven deepfake face swapping detection. In *Proceedings of the IEEE/CVF conference on computer vision and pattern recognition*, pp. 4490–4499, 2023.
- Huang, Z., Xia, B., Lin, Z., Mou, Z., and Yang, W. Ffaa: Multimodal large language model based explainable open-world face forgery analysis assistant. *arXiv preprint arXiv:2408.10072*, 2024.
- Jeong, J., Zou, Y., Kim, T., Zhang, D., Ravichandran, A., and Dabeer, O. Winclip: Zero-/few-shot anomaly classification and segmentation. In *Proceedings of the IEEE/CVF Conference on Computer Vision and Pattern Recognition (CVPR)*, pp. 19606–19616, June 2023.
- Jeong, Y., Kim, D., Ro, Y., and Choi, J. Frepgan: Robust deepfake detection using frequency-level perturbations. In *Proceedings of the AAAI conference on artificial intelligence*, volume 36, pp. 1060–1068, 2022.
- Khan, S. A. and Dang-Nguyen, D.-T. Clipping the deception: Adapting vision-language models for universal deepfake detection. In *Proceedings of the 2024 International Conference on Multimedia Retrieval*, pp. 1006–1015, 2024.
- Leng, S., Zhang, H., Chen, G., Li, X., Lu, S., Miao, C., and Bing, L. Mitigating object hallucinations in large vision-language models through visual contrastive decoding. In *Proceedings of the IEEE/CVF Conference on Computer Vision and Pattern Recognition*, pp. 13872–13882, 2024.
- Lester, B., Al-Rfou, R., and Constant, N. The power of scale for parameter-efficient prompt tuning. In *Proceedings of the 2021 Conference on Empirical Methods in Natural Language Processing*, pp. 3045–3059, 2021.
- Li, J., Li, D., Savarese, S., and Hoi, S. Blip-2: Bootstrapping language-image pre-training with frozen image encoders and large language models. In *International conference on machine learning*, pp. 19730–19742. PMLR, 2023.
- Li, L., Bao, J., Zhang, T., Yang, H., Chen, D., Wen, F., and Guo, B. Face x-ray for more general face forgery detection. In *Proceedings of the IEEE/CVF conference on computer vision and pattern recognition*, pp. 5001–5010, 2020a.
- Li, Y., Yang, X., Sun, P., Qi, H., and Lyu, S. Celeb-df: A large-scale challenging dataset for deepfake forensics. In *Proceedings of the IEEE/CVF conference on computer vision and pattern recognition*, pp. 3207–3216, 2020b.
- Liu, B., Liu, B., Ding, M., Zhu, T., and Yu, X. Ti2net: temporal identity inconsistency network for deepfake detection. In *Proceedings of the IEEE/CVF Winter Conference on Applications of Computer Vision*, pp. 4691–4700, 2023.
- Liu, H., Li, X., Zhou, W., Chen, Y., He, Y., Xue, H., Zhang, W., and Yu, N. Spatial-phase shallow learning: rethinking face forgery detection in frequency domain. In *Proceedings of the IEEE/CVF conference on computer vision and pattern recognition*, pp. 772–781, 2021.
- Liu, H., Li, C., Wu, Q., and Lee, Y. J. Visual instruction tuning. *Advances in neural information processing systems*, 36, 2024a.
- Liu, X., Ji, K., Fu, Y., Tam, W., Du, Z., Yang, Z., and Tang, J. P-tuning: Prompt tuning can be comparable to fine-tuning across scales and tasks. In *Proceedings of the 60th Annual Meeting of the Association for Computational Linguistics (Volume 2: Short Papers)*, pp. 61–68, 2022.
- Liu, X., Li, P., Huang, H., Li, Z., Cui, X., Liang, J., Qin, L., Deng, W., and He, Z. Fka-owl: Advancing multimodal fake news detection through knowledge-augmented lvlms. In *Proceedings of the 32nd ACM International Conference on Multimedia*, pp. 10154–10163, 2024b.
- Nguyen, D., Mejri, N., Singh, I. P., Kuleshova, P., Astrid, M., Kacem, A., Ghorbel, E., and Aouada, D. Laa-net: Localized artifact attention network for quality-agnostic

- and generalizable deepfake detection. In *Proceedings of the IEEE/CVF Conference on Computer Vision and Pattern Recognition*, pp. 17395–17405, 2024.
- Qian, Y., Yin, G., Sheng, L., Chen, Z., and Shao, J. Thinking in frequency: Face forgery detection by mining frequency-aware clues. In *European conference on computer vision*, pp. 86–103. Springer, 2020.
- Ramesh, A., Pavlov, M., Goh, G., Gray, S., Voss, C., Radford, A., Chen, M., and Sutskever, I. Zero-shot text-to-image generation. In *International conference on machine learning*, pp. 8821–8831. Pmlr, 2021.
- Rossler, A., Cozzolino, D., Verdoliva, L., Riess, C., Thies, J., and Nießner, M. Faceforensics++: Learning to detect manipulated facial images. In *Proceedings of the IEEE/CVF international conference on computer vision*, pp. 1–11, 2019.
- Selvaraju, R. R., Cogswell, M., Das, A., Vedantam, R., Parikh, D., and Batra, D. Grad-cam: Visual explanations from deep networks via gradient-based localization. In *Proceedings of the IEEE international conference on computer vision*, pp. 618–626, 2017.
- Shi, Z., Chen, H., Chen, L., and Zhang, D. Discrepancy-guided reconstruction learning for image forgery detection. In *Proceedings of the Thirty-Second International Joint Conference on Artificial Intelligence*, pp. 1387–1395, 2023.
- Shiohara, K. and Yamasaki, T. Detecting deepfakes with self-blended images. In *Proceedings of the IEEE/CVF Conference on Computer Vision and Pattern Recognition*, pp. 18720–18729, 2022.
- Su, Y., Lan, T., Li, H., Xu, J., Wang, Y., and Cai, D. Pandagpt: One model to instruction-follow them all. In *Proceedings of the 1st Workshop on Taming Large Language Models: Controllability in the era of Interactive Assistants!*, pp. 11–23, 2023.
- Sun, Y., Zhang, Z., Echizen, I., Nguyen, H. H., Qiu, C., and Sun, L. Face forgery detection based on facial region displacement trajectory series. In *Proceedings of the IEEE/CVF Winter Conference on Applications of Computer Vision*, pp. 633–642, 2023.
- Tan, C., Zhao, Y., Wei, S., Gu, G., Liu, P., and Wei, Y. Rethinking the up-sampling operations in cnn-based generative network for generalizable deepfake detection. In *Proceedings of the IEEE/CVF Conference on Computer Vision and Pattern Recognition*, pp. 28130–28139, 2024.
- Wang, P., Bai, S., Tan, S., Wang, S., Fan, Z., Bai, J., Chen, K., Liu, X., Wang, J., Ge, W., et al. Qwen2-vl: Enhancing vision-language model’s perception of the world at any resolution. *arXiv preprint arXiv:2409.12191*, 2024a.
- Wang, T., Liao, X., Chow, K. P., Lin, X., and Wang, Y. Deepfake detection: A comprehensive survey from the reliability perspective. *ACM Computing Surveys*, 2024b.
- Wang, Y., Yu, K., Chen, C., Hu, X., and Peng, S. Dynamic graph learning with content-guided spatial-frequency relation reasoning for deepfake detection. In *Proceedings of the IEEE/CVF Conference on Computer Vision and Pattern Recognition*, pp. 7278–7287, 2023a.
- Wang, Z., Bao, J., Zhou, W., Wang, W., and Li, H. Alt-freezing for more general video face forgery detection. In *Proceedings of the IEEE/CVF conference on computer vision and pattern recognition*, pp. 4129–4138, 2023b.
- Xu, Y., Liang, J., Jia, G., Yang, Z., Zhang, Y., and He, R. Tall: Thumbnail layout for deepfake video detection. In *Proceedings of the IEEE/CVF international conference on computer vision*, pp. 22658–22668, 2023.
- Xu, Z., Zhang, X., Li, R., Tang, Z., Huang, Q., and Zhang, J. Fakeshield: Explainable image forgery detection and localization via multi-modal large language models. *arXiv preprint arXiv:2410.02761*, 2024.
- Yan, Z., Zhang, Y., Fan, Y., and Wu, B. Ucf: Uncovering common features for generalizable deepfake detection. In *Proceedings of the IEEE/CVF International Conference on Computer Vision*, pp. 22412–22423, 2023.
- Yan, Z., Luo, Y., Lyu, S., Liu, Q., and Wu, B. Transcending forgery specificity with latent space augmentation for generalizable deepfake detection. In *Proceedings of the IEEE/CVF Conference on Computer Vision and Pattern Recognition*, pp. 8984–8994, 2024.
- Yang, R., Song, L., Li, Y., Zhao, S., Ge, Y., Li, X., and Shan, Y. Gpt4tools: Teaching large language model to use tools via self-instruction. *Advances in Neural Information Processing Systems*, 36, 2024.
- Zhao, H., Zhou, W., Chen, D., Wei, T., Zhang, W., and Yu, N. Multi-attentional deepfake detection. In *Proceedings of the IEEE/CVF conference on computer vision and pattern recognition*, pp. 2185–2194, 2021a.
- Zhao, T., Xu, X., Xu, M., Ding, H., Xiong, Y., and Xia, W. Learning self-consistency for deepfake detection. In *Proceedings of the IEEE/CVF international conference on computer vision*, pp. 15023–15033, 2021b.
- Zhou, K., Yang, J., Loy, C. C., and Liu, Z. Conditional prompt learning for vision-language models. In *IEEE/CVF Conference on Computer Vision and Pattern Recognition (CVPR)*, 2022.
- Zhu, D., Chen, J., Shen, X., Li, X., and Elhoseiny, M. MiniGPT-4: Enhancing vision-language understanding

with advanced large language models. In *The Twelfth International Conference on Learning Representations*, 2024.

A. You *can* have an appendix here.

You can have as much text here as you want. The main body must be at most 8 pages long. For the final version, one more page can be added. If you want, you can use an appendix like this one.

The `\onecolumn` command above can be kept in place if you prefer a one-column appendix, or can be removed if you prefer a two-column appendix. Apart from this possible change, the style (font size, spacing, margins, page numbering, etc.) should be kept the same as the main body.